Journal of Basic Physical Research ISSN: 2141-8403 Prints, 2141-8411 Online
Vol.14, Issue 2, October, 2025, pp. 10 – 21, Available online at https://journals.unizik.edu.ng/jbpr/

AN X-RAY DIFFRACTION ANALYSIS OF CEMENT STABILIZED E-WASTE CONTAMINATED SOIL: (A CASE STUDY OF ALABA INTERNATIONAL MARKET, LAGOS STATE, NIGERIA)

Ugochukwu Tochukwu Ernest*[1], Amu Olugbenga Oludolapo[1], Olaniyan Amo[2], Oko Chukwuka[3], Okomba Nnamdi Stephen
[1]*Department of Civil Engineering, Faculty of Engineering, Federal University Oye-Ekiti, Ekiti State, Nigeria.*
[2]*Department of Agriculture and Bio-Resources Engineering, Faculty of Engineering, Federal University Oye-Ekiti, Ekiti State, Nigeria.*
[3]*Nigerian Building and Road Research Institute, Abuja, Nigeria*
[4]*Department of Computer Engineering, Faculty of Engineering, Federal University Oye-Ekiti, Ekiti State, Nigeria.*
***Corresponding author:** ernest.ugochukwu@fuoye.edu.ng

Abstract
This study examines the mineralogical transformations in e-waste contaminated soils (CO1, CO2 and CO3) treated with cement contents at 0,2,4,6,8 and 10 percentages using X-ray diffraction (XRD) analysis. The e-waste soil samples (CO1, CO2, and CO3) were obtained from three diifferent sites at St Patrick Catholic Church, Sunny Bus Stop and Kpako Area of Alaba International Market, Lagos State, Nigeria. Disturbed soil Samples was obtained at a depth of not less than 2m. The objective of this paper is to understand the phase evolution and the formation of hydration products at different cement addition and to establish the optimum of the addictives on these e-waste soil samples and to determine how cement hydration products contribute to heavy metal immobilization, thereby reducing leachability and safeguarding groundwater quality within the area. The results indicate a progressive transformation of mineral phases. The untreated soil contained Quartz (SiO_2), Calcite ($CaCO_3$), Lead Oxide (PbO), and Copper Oxide (CuO) across all the soil samples. With cement addition, Calcium Hydroxide ($Ca(OH)_2$) and Calcium Silicate Hydrate (C-S-H) emerged, indicating hydration reactions. At 6% cement, maximum mineral transformation occurred with the formation of C-A-S-H and gehlenite ($Ca_2Al(AlSi)O_7$), enhancing soil stabilization. Beyond 6%, hydration activity declined. These results suggest that 6% cement optimally stabilizes e-waste soil of all the treated e-waste contaminated soil, improving its geotechnical and environmental properties of e-waste-contaminated soils, contributing to sustainable soil remediation efforts and given more value to the soil to be used for construction purposes especially in Alaba area of Lagos State, Nigeria where the soil abounds.
Keywords: *E-waste soil, Cement stabilization, X-ray Diffraction (XRD)*

Introduction

The increasing generation of electrical and electronic waste (e-waste) has become a very pressing environmental concern all over the word as a result of its hazardous nature due to the presence of heavy metals and toxic chemicals which leaches into the soil and results to severe degradation of its environment and potential negative impacts on soils engineering properties as a result of improper disposal.

In Nigeria, traditional disposal methods are used as seen in plate 1 and it is inadequate in preventing e-waste contamination on the surrounding soils. In Alaba area that provides the largest electronic and electrical market in west Africa, these electronic equipment that are beyond repair are dumped in a site and burnt, over the years the components of the gadgets decompose and leach into the soil and affects the ground water beneath it.

E-waste primarily consists of discarded electronic devices such as televisions, refrigerators, computers, and mobile phones. These materials contain toxic elements, including lead (Pb), copper (Cu), cadmium (Cd), and nickel (Ni), which can leach into the soil and groundwater,

posing environmental and health risks (Robinson, 2009). The improper disposal and dismantling of e-waste, especially in developing countries, exacerbate soil contamination.

Soil stabilization involves modifying soil properties to improve strength and durability. Various stabilization methods include mechanical stabilization, chemical stabilization (using lime, fly ash, or cement), and bio-stabilization (Sabat, 2012). Cement stabilization, in particular, is widely used due to its effectiveness in immobilizing contaminants and enhancing soil mechanical properties (Al-Amoudi et al., 2017). When cement is added to soil, hydration reactions occur, leading to the formation of compounds such as calcium silicate hydrate (C-S-H) and calcium aluminum silicate hydrate (C-A-S-H). These compounds enhance soil cohesion and encapsulate heavy metals, reducing their mobility (Fernandez et al., 2016). The Cement stabilization is a widely employed technique to improve soil properties and immobilize hazardous elements (Al-Amoudi et al., 2017).

Cement plays a critical role in stabilizing e-waste contaminated soils by binding heavy metals and hazardous materials into a stable matrix. The hydration process of cement produces calcium silicate hydrate (C-S-H) and calcium hydroxide (Portlandite), which can encapsulate contaminants and reduce their mobility. Cement also increases the pH of the soil, causing the precipitation of certain heavy metals as insoluble hydroxides, further reducing their potential leaching. Several studies have demonstrated the efficacy of cement in stabilizing soils contaminated with heavy metals, including lead, cadmium, and chromium. For instance, Conner and Hoeffner (1998) found that the use of Portland cement could significantly reduce the leachability of heavy metals in contaminated soils thereby reducing its negative effect on its engineering properties. In the context of e-waste, cement can effectively bind and immobilize metals found in electronic components, such as lead from CRT monitors, cadmium from batteries, and copper from wiring.

X-ray diffraction (XRD) is one of the analytical technique tools used to identify mineral phases in soil samples especially in e-waste soil sample. The presence of crystalline structures and track mineralogical transformations can be observed by analyzing diffraction patterns due to stabilization processes (Zhang et al., 2018). In cement treated e-waste contaminated soils, XRD analysis helps identify hydration products such as portlandite ($Ca(OH)_2$), ettringite ($Ca_6Al_2(SO_4)_3(OH)_{12}•26H_2O$), and C-S-H, which contribute to improved soil stability (Wen et al., 2019). The progressive mineralogical changes observed through XRD provide insights into the effectiveness of cement stabilization in reducing heavy metal mobility and enhancing soil strength. This study focuses on the X-ray diffraction (XRD) analysis of an e-waste-contaminated soil samples (CO1, CO2 and CO3) treated with different cement percentages to determine the mineralogical changes that occur upon stabilization.

This study investigates mineralogical changes in e-waste contaminated soils from Alaba International Market following cement stabilization, using X-ray diffraction to assess phase transformations. The work aims to determine how cement hydration products contribute to heavy metal immobilization, thereby reducing leachability and safeguarding groundwater quality within the area.



***Plate 1**: E- waste handling in Nigeria*

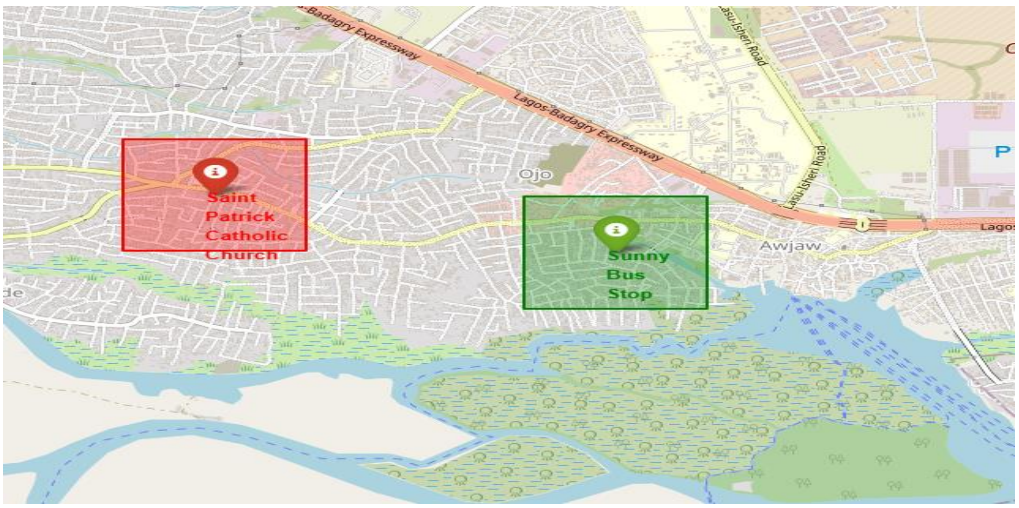

***Figure 1:** Map of Ojo Local Government showing Alaba research area*

The Study Area

Lagos State, located in the southwestern part of Nigeria, is characterized by a unique geological setting that plays a significant role in its environmental and infrastructural development. The state's geology is primarily shaped by its coastal location along the Gulf of Guinea, with a landscape dominated by sedimentary formations, coastal plains, lagoons, and creeks. Ojo Alaba is situated near the Lagos lagoon, by the Badagry Expressway, around 20 kilometers from the Lagos city center. It spans a few neighborhoods like Alaba Rago, Alaba Onilu, Alaba Isale Oko, and Alaba Suru in Ojo. The area lies on the geographic coordinates of latitude 6.4500° N and longitude 3.2000° E. The area has a tropical wet climate, very hot and humid most of the year with two rainy seasons. Due to its proximity to the lagoon, it experiences moderate to high rainfall. It is low-lying and susceptible to flooding during the peak rainy season because of poor drainage infrastructure. Ojo Alaba is best known as the hub of international trade and technological markets in Nigeria. The International Trade Fair complex located here hosts major consumer goods trade fairs annually that attract traders from within and outside Nigeria. The Alaba International Market is the largest electronics market in Africa. All kinds of electronics, from household appliances, mobile phones, televisions, generators, audio devices, to spare parts are traded here. Most goods are sourced from Asia and sold at wholesale and retail prices to traders who supply across West Africa. Thousands

of local and foreign traders operate in this market generating huge revenues. Associated markets like Alaba Suru market have also emerged around Alaba International market.

Materials and Methods

Materials

The materials used were: e-waste contaminated soil sample (CO1, CO2 and CO3), Portland cement and water.

E-waste Contaminated Soil Sample (CO1): The e-waste contaminated soil samples were collected from three locations within Alaba International Market, Ojo, Lagos State, Nigeria. Sample **CO1** was obtained from the Kpako area, **CO2** from St. Patrick Catholic Church, and **CO3** from Sunny Bus Stop.

These sites predominantly contain discarded televisions, refrigerators, electrical cables, and mobile phones. Sampling was carried out at depths not less than 2 m below the ground surface to avoid surface contamination and capture the more representative subsoil layer.

A **disturbed sampling technique** was employed, in which soil was excavated without preserving its natural structure but ensuring that the representative composition of the material was retained for subsequent mineralogical and chemical analyses in the laboratory. The samples were labeled correctly, indicating the soil description, sampling depth and date.

Portland cement: This was obtained from an open market in Keyentta Area of Enugu State, Nigeria.

Water: The water used was obtained from the running taps in the laboratory; the source was borehole. Distilled water was not used so as to obtain results that would reflect in-situ conditions.

Methods

The e-waste contaminated soil samples were air-dried, pulverized, and sieved through a 2 mm sieve to remove large debris and ensure uniformity and was treated with cement at varying percentages (0%, 2%, 4%, 6%, 8%, 10%). The e-waste soil samples were oven-dried at **105–110 °C** to remove all moisture content, thereby preventing interference from water molecules during X-ray diffraction (XRD) analysis and ensuring accurate identification of mineral phases. After drying, the samples were ground into fine powder to achieve a uniform particle size, which improves the quality and resolution of the XRD diffraction patterns. Both the **natural (untreated)** e-waste contaminated soil samples and the **cement-stabilised** samples were prepared in this way. For the cement-stabilised samples, curing was carried out for **28 days** under controlled moisture conditions before oven drying and grinding, to allow sufficient time for cement hydration and pozzolanic reactions to occur prior to mineralogical testing.

The soil samples were then mounted on an XRD sample holder. The XRD Testing Procedure was done with the X-ray diffractometer with Cu-Kα radiation, Scan Range of 5° to 70° (2θ range) and a 0.02° step size while the operating conditions used was 40 kV, 30 mA.

The diffractogram was analyzed using HighScore Plus software to identify mineral phases and peak was compared with reference patterns from the ICDD database to detect stabilization-related minerals (quartz, calcite, portlandite, ettringite, C-S-H, etc.). The changes in mineral composition are examined to assess the chemical reactions and stabilization effects of cement on the e-waste soil samples (CO1, CO2 and CO3). The oxide composition of the e-waste soil and Portland cement was determined using X-ray fluorescence (XRF) in accordance with **BS EN 196-2:2013**, which involves irradiating finely ground samples with X-rays to measure characteristic fluorescent emissions for rapid multi-element quantification.

Results and Discussion

Table 1: Summary of the chemical composition of the Portland cement used in the laboratory

Oxide	Symbol
Calcium oxide	CaO
Silicon dioxide	SiO_2
Aluminium oxide	Al_2O_3
Ferric oxide	Fe_2O_3
Magnesium oxide	MgO
Sulphur trioxide	SO_3
Potassium oxide	K_2O
Sodium oxide	Na_2O

Table 2: Summary of all XRD test result for e-waste soil samples CO1, CO2 and CO3 before treatment

Soil Sample	Mineral Phase	2θ (degrees)	d-Spacing (Å)	Relative Intensity
CO1	SiO_2, $CaCO_3$, PbO, CuO, SiO_2	26.6, 29.4, 28.5, 35.5, Broad peak ~22	3.34, 3.04, 3.13, 2.52, 4.1	1000,700,300,200, 400
CO2	SiO_2, $CaCO_3$, PbO, CuO, SiO_2,SiO_2	26.6, 29.4, 28.5, 35.5, 20.8, Broad peak ~22	3.34, 3.04, 3.13, 2.52, 4.27, 4.04	1000,700,500,400, 450, 400
CO3	SiO_2, $CaCO_3$, PbO, CuO, SiO_2	26.6, 29.4, 28.5, 35.5, 20.8	3.34, 3.04, 3.13, 2.52, 4.27	1000,600,500,450, 400

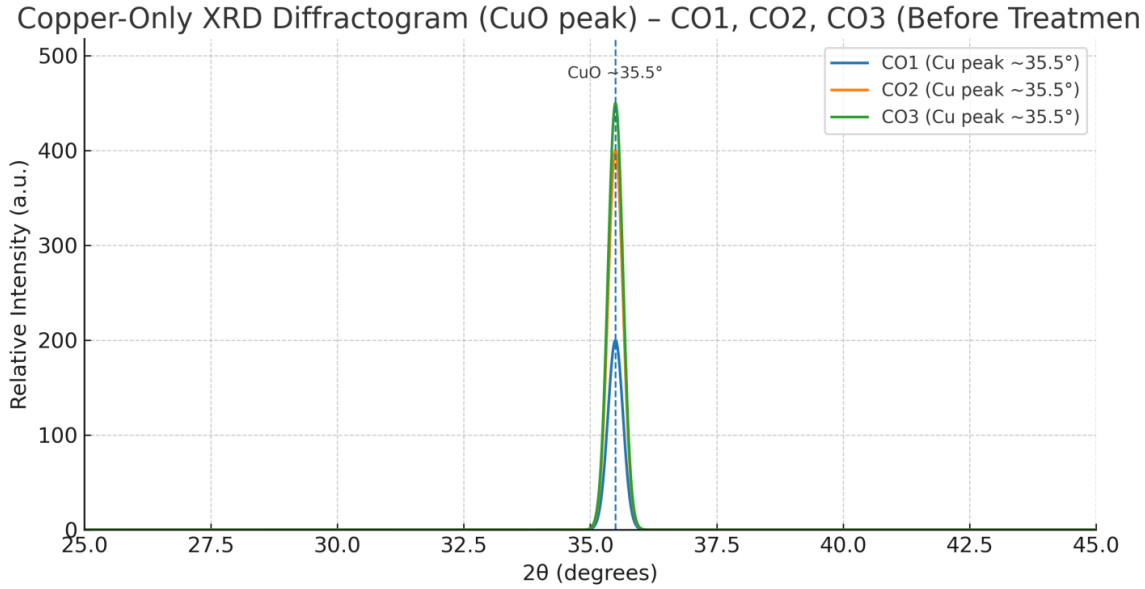

Figure 2: *XRD Diffractogram for Copper only (CO1, CO2 & CO3) before treatment*

Table 3: Summary of all XRD test result for e-waste soil samples CO1 treated with cement (Kpako Dump Site)

Soil Sample	Cement (%)	Mineral Phase	2θ (degrees)	d-Spacing (Å)	Relative Intensity
CO1	0	SiO_2, $CaCO_3$, PbO, CuO, SiO_2	26.6, 29.4, 28.5, 35.5, Broad peak ~22	3.34, 3.04, 3.13, 2.52, 4.1	1000,700,300,200, 400
	2	SiO_2, $CaCO_3$, $Ca(OH)_2$, C-S-H	26.6, 29.5, 18.1, 32.5	3.34, 3.02, 4.89, 2.76	900,650,450,300
	4	SiO_2, $CaCO_3$, $Ca(OH)_2$, $Ca_6Al_2(SO_4)_3(OH)_{12}\cdot 26H_2O$	26.6, 29.5, 18.1, 9.1	3.34, 3.02, 4.89, 9.70	800,600,500,250
	6	SiO_2, $CaCO_3$, $Ca(OH)_2$, C-S-H, C-A-S-H, $Ca_2Al(AlSi)O_7$, SiO_2	26.6, 29.5, 18.1, 32.5, 30.5, 32.2, Broad peak ~22	3.34, 3.02, 4.89, 2.76, 2.92, 2.78, 4.1	750,500,700,800, 700,400,600
	8	SiO_2, $CaCO_3$, $Ca(OH)_2$, C-S-H	26.6, 29.5, 18.1, 32.5	3.34, 3.02, 4.89, 2.76	700,450,500,500
	10	SiO_2,$Ca(OH)_2$, C-S-H, SiO_2	26.6, 18.1, 32.5, Broad peak ~22	3.34, 4.89, 2.76, 4.1	650,400,400,500

Table 4: Summary of all XRD test result for e-waste soil samples CO2 treated with cement (Behind St Patrick Catholic Church)

Soil Sample	Cement (%)	Mineral Phase	2θ (degrees)	d-Spacing (Å)	Relative Intensity
CO2	0	SiO_2, $CaCO_3$, PbO, CuO, SiO_2,SiO_2	26.6, 29.4, 28.5, 35.5, 20.8, Broad peak ~22	3.34, 3.04, 3.13, 2.52, 4.27, 4.04	1000,700,500, 400, 450, 400
	2	SiO_2, $CaCO_3$, $Ca(OH)_2$, C-S-H, $Ca_6Al_2(SO_4)_3(OH)_{12}\cdot 26H_2O$	26.6, 29.5, 18.1, 32.5,9.1	3.34, 3.02, 4.89, 2.76, 9.70	900,650,400,300, 250
	4	SiO_2, $CaCO_3$, $Ca(OH)_2$, C-S-H, $Ca_6Al_2(SO_4)_3(OH)_{12}\cdot 26H_2O$	26.6, 29.5, 18.1,32.5, 9.1	3.34, 3.02, 4.89,2.76, 9.70	850,600,500,400, 300
	6	SiO_2, $CaCO_3$, $Ca(OH)_2$, C-S-H, C-A-S-H, $Ca_2Al(AlSi)O_7$, SiO_2	26.6, 29.5, 18.1, 32.5, 30.5, 32.2, 22.0 (broad)	3.34, 3.02, 4.89, 2.76, 2.92, 2.78, 4.04	800,550,700,800, 700,500,400
	8	SiO_2, $CaCO_3$, $Ca(OH)_2$, C-S-H, $Ca_6Al_2(SO_4)_3(OH)_{12}\cdot 26H_2O$	26.6, 29.5, 18.1, 32.5, 9.1	3.34, 3.02, 4.89, 2.76, 9.70	850,500,600,500, 300
	10	SiO_2, $CaCO_3$,$Ca(OH)_2$, C-S-H, SiO_2	26.6, 29.5,18.1, 32.5, Broad peak ~22	3.34, 3.02,4.89, 2.76, 4.04	800,400,450,450, 350

Table 5: Summary of all XRD test result for e-waste soil samples CO3 treated with cement (Sunny Bus Stop)

Soil Sample	Cement (%)	Mineral Phase	2θ (degrees)	d-Spacing (Å)	Relative Intensity
CO3	0	SiO_2, $CaCO_3$, PbO, CuO, SiO_2	26.6, 29.4, 28.5, 35.5, 20.8	3.34, 3.04, 3.13, 2.52, 4.27	1000,600,500,450, 400
	2	SiO_2, $CaCO_3$, $Ca(OH)_2$, C-S-H, $Ca_6Al_2(SO_4)_3(OH)_{12}\cdot 26H_2O$	26.6, 29.5, 18.1, 32.5,9.1	3.34, 3.02, 4.89, 2.76, 9.70	950,550,500,400, 300
	4	SiO_2, $CaCO_3$, $Ca(OH)_2$, C-S-H, $Ca_6Al_2(SO_4)_3(OH)_{12}\cdot 26H_2O$	26.6, 29.5, 18.1,32.5, 9.1	3.34, 3.02, 4.89,2.76, 9.70	900,500,600,500, 400
	6	SiO_2, $CaCO_3$, $Ca(OH)_2$, C-S-H, C-A-S-H, $Ca_2Al(AlSi)O_7$	26.6, 29.5, 18.1, 32.5, 30.5, 32.2	3.34, 3.02, 4.89, 2.76, 2.92, 2.78	850,400,800,900, 750,500
	8	SiO_2, $CaCO_3$, $Ca(OH)_2$, C-S-H, $Ca_6Al_2(SO_4)_3(OH)_{12}\cdot 26H_2O$	26.6, 29.5, 18.1, 32.5, 9.1	3.34, 3.02, 4.89, 2.76, 9.70	800,450,550,600, 300
	10	SiO_2, $CaCO_3$,$Ca(OH)_2$, C-S-H, SiO_2	26.6, 29.5,18.1, 32.5, Broad peak ~22	3.34, 3.02,4.89, 2.76, 4.04	750,400,450,500, 400

Table 1 shows the primary oxides identified in the Portland cement used for the laboratory tests. The dominant constituent is calcium oxide (CaO), which is the main source of lime in cement and is responsible for the formation of calcium silicate hydrates (C–S–H) during hydration, the primary phase contributing to strength development. Silicon dioxide (SiO_2) combines with CaO to form C–S–H, while aluminium oxide (Al_2O_3) and ferric oxide (Fe_2O_3) participate in forming calcium aluminates and ferrites, which influence setting time and early strength.

Minor constituents such as magnesium oxide (MgO) can contribute to soundness if present in small amounts but may cause expansion problems at higher levels. Sulphur trioxide (SO_3) is typically introduced via gypsum addition and plays a crucial role in controlling setting time. Potassium oxide (K_2O) and sodium oxide (Na_2O) are alkalis that can influence alkali–silica reactions if reactive aggregates are present, although in low percentages they have minimal effect. Overall, this aligns with the chemical composition of a typical profile of ordinary Portland cement specified in ASTM C150 and is suitable for soil stabilisation purposes (Neville, 2011).

Overall, the oxide composition shown in Table 1 reflects the typical chemical profile of Portland cement suitable for soil stabilisation, providing the necessary lime content for pozzolanic reactions and hydration product formation that improve soil engineering properties.

Table 2 shows the X-ray diffraction (XRD) analysis for the untreated e-waste contaminated soil samples CO1, CO2, and CO3 which reveals a consistent presence of key mineral phases, with variations in intensity and d-spacing, indicating heterogeneous mineralogical composition across the samples. The major crystalline phases detected include Silicon dioxide (SiO_2), the detection of calcium carbonate ($CaCO_3$) in the untreated soil indicates the presence of natural or anthropogenic carbonates, but without quantitative analysis it cannot be classified as calcareous. Other key mineral phases are lead oxide (PbO), and Copper oxide (CuO) as shown in figure 2

Silicon Dioxide (SiO_2), identified at $2\theta \approx 26.6°$, with a d-spacing of 3.34 Å and highest relative intensity (1000), was the dominant peak in all samples. This phase is typical of quartz, a highly crystalline and stable form of silica commonly found in natural soils and associated with the breakdown of electronic glass components such as cathode ray tubes and printed circuit boards (Wang et al., 2021). The consistent presence of broad peaks around 22° further suggests the occurrence of amorphous silica, which may originate from glassy waste materials or degraded silicates in e-waste, such as glass from cathode ray tubes (CRTs) or ceramics from electronic components. Calcium carbonate ($CaCO_3$), detected at $2\theta \approx 29.4°$ with a d-spacing of 3.04 Å, is prevalent across all samples. It is associated with the calcite form of limestone, which may originate from the plastic fillers and coating materials used in electronic devices (Sabat, 2012). Its significant presence may influence the buffering capacity and chemical reactivity of the soil.

Lead Oxide (PbO) appeared at $2\theta \approx 28.5°$ with d-spacing 3.13 Å, especially strong in CO2 and CO3 (relative intensities 500 and 500 respectively). This is a notable indicator of toxic contamination, typically arising from solder, batteries, and cathode ray tube (CRT) glass (Ghosh et al., 2020). PbO's presence confirms the e-waste origin and reinforces the hazardous nature of the contaminated soil, requiring stabilization before any beneficial reuse. Copper Oxide (CuO) At $2\theta \approx 35.5°$ and d-spacing 2.52 Å, CuO was detected in all samples with relatively lower intensities (200–450). CuO is commonly derived from oxidized circuit boards

and wire coatings and is a strong indicator of e-waste pollution (Wen et al., 2019). Its relatively lower intensity suggests partial oxidation or lesser concentration compared to SiO_2 and $CaCO_3$.

CO2 and CO3 show additional SiO_2 peaks around $2\theta \approx 20.8°$ and broad peaks near 22°, with d-spacing values of 4.27 Å and 4.04 Å, suggesting a mix of amorphous and crystalline silica phases. These phases could result from fine glassy particles and thermally degraded silicates in the e-waste material (Alhassan et al., 2020).

CO2 exhibits the most complex profile, with six mineral phases and the highest number of SiO_2-related peaks. This implies higher variability or more diverse contamination sources in this sample while CO1 shows more dominant crystalline peaks with slightly higher intensity for $CaCO_3$ and PbO compared to CO3, suggesting variability in mineral distribution. All samples consistently show hazardous oxides (PbO, CuO), indicating the necessity for treatment/stabilization to prevent leaching and environmental risks.

The absence of iron and aluminium oxides in the natural e-waste contaminated soil may be due to the dominance of silica and carbonate rich materials from e-waste, the possible presence of Fe and Al in amorphous forms undetectable by XRD, masking by strong quartz and calcite peaks, and potential leaching from acidic e-waste leachates reducing their concentrations below detection limits.

Table 3 shows the XRD results of e-waste-contaminated soil sample CO1 which shows significant mineralogical transformations with increasing cement content. Initially, at **0% cement**, the dominant minerals are **quartz (SiO_2), calcite ($CaCO_3$), lead oxide (PbO), copper oxide (CuO), and an amorphous silica phase**. The presence of PbO and CuO indicates contamination from e-waste materials, particularly from discarded electronics such as televisions and refrigerators (Wen et al., 2019). Upon adding **cement (2% to 10%)**, new hydration products appear, such as **Calcium hydroxide ($Ca(OH)_2$)**, a byproduct of cement hydration. **Calcium silicate hydrate (C-S-H)**, a primary strength-giving phase. **Calcium aluminate sulfate hydrate (C-A-S-H)**, formed at 6% cement, indicating increased pozzolanic reactions and **Ettringite ($Ca_6Al_2(SO_4)_3(OH)_{12}•26H_2O$)**, The appearance of $Al_2(SO_4)_3$ in cement stabilised soils, absent in the untreated samples, is likely due to the reaction between aluminium bearing phases in cement (e.g., Al_2O_3 from C_3A) and sulphates (SO_3 from gypsum), possibly with minor contributions from sulphur-containing e-waste residues and the sulfate containing phase wsa at 4% cement. These findings align with **Dauda et al. (2018)**, who studied e-waste-contaminated soils stabilized with cement and lime. They observed similar mineral transformations, where SiO_2 remained a dominant phase while **$Ca(OH)_2$ and C-S-H** formed progressively with higher cement content. They also identified the gradual disappearance of heavy metal oxides due to their interaction with cementitious phases, a phenomenon seen in this study as PbO and CuO peaks diminish at higher cement contents. Likewise, **Al-Amoudi et al. (2017)** found that cement stabilized contaminated soils exhibited high formation of **C-S-H and C-A-S-H,** which contributed to heavy metal immobilization and soil strength development.

The XRD results showing **C-S-H, $Ca(OH)_2$, and C-A-S-H** phases match findings by **Fernandez et al. (2016)**, who examined the pozzolanic activity of calcined clay minerals. They reported that hydration of calcium-based materials with siliceous components led to the formation of **C-S-H and C-A-S-H**, which contribute to long-term soil stabilization. At 6% cement, the study identifies the appearance of **$Ca_2Al(AlSi)O_7$**, which is consistent with **Wen et al. (2019)**, who found that such mineral phases enhance the binding capacity of heavy

metals, reducing their mobility. This study further confirms that cementitious phases such as **C-S-H and ettringite effectively encapsulate heavy metals**, thereby reducing environmental risks. The XRD results demonstrate that at **10% cement**, dominant peaks include **SiO_2, C-S-H, and $Ca(OH)_2$,** while ettringite and C-A-S-H disappear. This pattern is also observed by **Robinson (2009)**, who suggested that excessive cement content leads to over-saturation of calcium hydroxide, reducing further pozzolanic reactions. Similarly, **Schluep et al. (2009)** highlighted that the optimal cement content for contaminated soil stabilization is typically between **4% and 8%,** beyond which excessive calcium hydroxide formation can limit further strength gains.

Table 4 presents the XRD analysis of e-waste contaminated soil sample CO2 treated with varying percentages of cement. The results reveal progressive mineralogical changes as cement content increases, indicating the chemical transformation of the soil matrix due to cement hydration and pozzolanic reactions.

At 2% and 4% cement, new hydration products appear such as Calcium hydroxide ($Ca(OH)_2$), also known as portlandite, with peak at ~18.1° (d = 4.89 Å), Calcium silicate hydrate (C-S-H), a poorly crystalline phase responsible for strength gain, appearing around 32.5° (d ≈ 2.76 Å) and Ettringite ($Ca_6Al_2(SO_4)_3(OH)_{12}•26H_2O$), identified at 9.1° (d ≈ 9.70 Å), indicating sulfate reaction from cement or e-waste components (Sabat, 2012; Ghosh et al., 2020).

At 6% cement, the peak intensities of hydration products increase significantly, C-A-S-H and Gehlenite ($Ca_2Al(AlSi)O_7$) are observed, indicating ongoing secondary reactions involving alumino-silicates and calcium ions. Persistence of SiO_2 and $CaCO_3$ suggests partial reaction of the original minerals, while the appearance of multiple binding phases marks this as a chemically active and stable blend, often linked with peak strength and durability (Alhassan et al., 2020).

At 8% and 10% cement content, the XRD patterns still exhibit the characteristic peaks of C–S–H, $Ca(OH)_2$, and ettringite; however, the reduced peak intensities for some hydration products indicate a possible decrease in their crystallinity and relative abundance, This may suggest either: Saturation of reactive phases or over dosage of cement, where excess $Ca(OH)_2$ remains unreacted, potentially weakening long-term stability (Wen et al., 2019).

Table 5 shows he XRD analysis of sample CO3 reveals important mineralogical changes as cement content increases from 0% to 10%, indicating effective stabilization and pozzolanic reactions: At 2–4% Cement: New cement hydration products begin to form, notably Calcium Hydroxide ($Ca(OH)_2$) and Calcium Silicate Hydrate (C-S-H), the primary binding phase responsible for strength gain in cement-treated soils. Additionally, the presence of ettringite ($Ca_6Al_2(SO_4)_3$ $(OH)_{12}·26H_2O$) indicates an early sulfate reaction. These reactions improve the soil's binding structure (Ghosh et al., 2020; Amu et al., 2011) while at 6% Cement (Peak Performance Phase): A richer phase development is observed with increased intensity of C-S-H and Calcium-Alumino-Silicate-Hydrate (C-A-S-H), along with Gehlenite ($Ca_2Al(AlSi)O_7$), signifying advanced pozzolanic reactions and aluminum incorporation. This supports the highest strength gain observed in cement-treated soils (Alhassan & Mustapha, 2007). The intensified peaks at $2\theta = 30.5°$ and 32.2° suggest enhanced crystalline structure and bonding.

At 8% Cement: The pattern is similar to 6%, with sustained presence of C-S-H and ettringite, though some relative peak intensities reduce, suggesting a diminishing marginal effect of excess cement. Overstabilization can hinder optimal performance due to excessive $Ca(OH)_2$

formation without adequate pozzolanic material (Muntohar & Hantoro, 2000) and At 10% Cement:
While C-S-H remains prominent, the appearance of a broad SiO_2 peak (~22°) may indicate partial amorphization or unreacted silica. Continued increase in cement does not yield new dominant phases, implying a stabilization saturation point. This aligns with common findings that 6–8% cement is optimal for cost-effective stabilization (Amu et al., 2011)

Conclusions

X-ray diffraction analysis of untreated e-waste contaminated soils (CO1, CO2, CO3) revealed dominant quartz (SiO_2) and calcite ($CaCO_3$) phases, with hazardous PbO and CuO residues indicating significant heavy metal contamination, the absence of Fe and Al oxides suggests limited natural attenuation potential.

Cement stabilization induced progressive formation of portlandite [$Ca(OH)_2$], calcium silicate hydrate (C-S-H), calcium aluminate silicate hydrate (C-A-S-H), and ettringite [$Ca_6Al_2(SO_4)_3(OH)_{12}\cdot 26H_2O$], especially at 4–8 % cement content. These hydration products are known to encapsulate heavy metals within low solubility phases and fill pore spaces, thereby reducing permeability and leachability.

From an environmental standpoint, the transformation of PbO and CuO into less mobile forms, coupled with reduced pore connectivity, indicates strong potentials for groundwater protection in e-waste affected sites. The results support the feasibility of cement-based stabilization as a low-cost, locally available, and technically viable remediation strategy for informal dumpsites in Lagos and similar settings. Optimal cement contents (4–8 %) balance mineralogical immobilization with material cost, suggesting practical applicability in large-scale soil remediation programs.

Acknowledgment

The authors would like to thank A.N Nnamani & Co for the assitannce in sample collection and Jubaz Engineering Services for their assistance with the sample preparation and testing.

References

Al-Amoudi, O. S. B., Maslehuddin, M., & Shameem, M. (2017). Stabilization of contaminated soil using cementitious materials: A review. *Journal of Materials in Civil Engineering, 29*(9), 04017107.

Alhassan, M., Amu, O. O., & Moses, G. (2020). Solidification/stabilization of e-waste contaminated lateritic soil using cement and pozzolans. *Journal of Environmental Engineering and Science*, 15(1), 12–21. https://doi.org/10.1139/jees-2020-0002

Alhassan, M., & Mustapha, A. M. (2007). *Effect of rice husk ash on cement stabilized laterite*. Leonardo Electronic Journal of Practices and Technologies, 6(11), 47–58.

Amu, O. O., Ogunniyi, S. A., & Oladeji, O. O. (2011). *Geotechnical properties of lateritic soil stabilized with sugarcane straw ash*. American Journal of Scientific and Industrial Research, 2(2), 323–331. https://doi.org/10.5251/ajsir.2011.2.2.323.331

Dauda, T., Akinwumi, I., & Ogunbode, E. (2018). Geotechnical behavior of e-waste-contaminated soil stabilized with cement and lime. *Construction and Building Materials, 188*, 361–372.

Fernandez, R., Martirena, F., & Scrivener, K. L. (2016). The origin of the pozzolanic activity of calcined clay minerals: A comparison between kaolinite, illite, and montmorillonite. *Cement and Concrete Research, 101*, 1–13.

Ghosh, A., Ghosh, P., & Chakraborty, S. (2020). *Effect of lime and cement on the strength and microstructure of e-waste contaminated soil*. International Journal of Geotechnical Engineering, 14(2), 184–192. https://doi.org/10.1080/19386362.2018.1485295

Ghosh, A., Ghosh, S., & Nath, S. (2020). Stabilization of e-waste contaminated soils using industrial by-products: A geotechnical and environmental perspective. *Journal of Hazardous Materials*, 393, 122385. https://doi.org/10.1016/j.jhazmat.2020.122385

Muntohar, A. S., & Hantoro, G. (2000). *Influence of rice husk ash and lime on engineering properties of a clayey subgrade*. Electronic Journal of Geotechnical Engineering, 5.

Robinson, B. H. (2009). E-waste: An assessment of global production and environmental impacts. *Science of the Total Environment, 408*(2), 183–191.

Sabat, A. K. (2012). Stabilization of expansive soil using waste ceramic dust. *Electronic Journal of Geotechnical Engineering, 17*(Z), 3915–3926

Schluep, M., Hagelüken, C., Meskers, C. E. M., & others. (2009). Market potential of innovative e-waste recycling technologies in developing countries. *Journal of Industrial Ecology, 13*(4), 592–610.

Wang, J., Wang, H., Wei, L., Chen, H., & Liu, Y. (2021). Mineralogical characterization and heavy metal behavior of e-waste contaminated soil. *Environmental Geochemistry and Health*, 43(2), 781–793. https://doi.org/10.1007/s10653-020-00602-4

Wen, B., Hu, X., Liu, Y., Wang, W., Feng, X., & Sridhar, B. (2019). Microstructural characteristics and heavy metal immobilization mechanisms in cement-treated contaminated soils. *Environmental Science & Technology, 53*(5), 2565–2573